Heavy quark dynamics via the Gribov-Zwanziger approach

Sumit,[1,*] Arghya Mukherjee,[2,†] Najmul Haque,[3,‡] and Binoy Krishna Patra[1,§]
[1]*Department of Physics, Indian Institute of Technology Roorkee, Roorkee 247667, India*
[2]*Ramakrishna Mission Residential College (Autonomous), Narendrapur, Kolkata-700103, India*
[3]*School of Physical Sciences, National Institute of Science Education and Research, An OCC of Homi Bhabha National Institute, Jatni-752050, India*

(Received 13 January 2024; accepted 2 June 2024; published 28 June 2024)

In this work, we investigate the momentum-dependent drag and diffusion coefficient of heavy quarks (HQs) moving in the quark-gluon plasma background. The leading order scattering amplitudes required for this purpose have been obtained using the Gribov-Zwanziger propagator for the mediator gluons to incorporate the nonperturbative effects relevant to the phenomenologically accessible temperature regime. The drag and diffusion coefficients so obtained have been implemented to estimate the temperature and momentum dependence of the energy loss of the HQ as well as the temperature dependence of the specific shear viscosity (η/s) of the background medium. Our results suggest a higher energy loss of the propagating HQ compared to the perturbative estimates, whereas the η/s is observed to comply with the AdS/CFT estimation over a significantly wider temperature range compared to the perturbative expectation.

DOI: 10.1103/PhysRevD.109.114043

I. INTRODUCTION

The ultimate aim of the ongoing experiments, namely the Relativistic Heavy Ion Collider (RHIC) at Brookhaven National Laboratory and Large Hadron Collider (LHC) at the European Council for Nuclear Research (CERN), is to create and study the new state of matter where bulk properties of this matter are governed by light quarks and gluons [1,2]. It is now widely proven that this new state, which is the deconfined state of quarks and gluons known as strongly interacting quark-gluon plasma (sQGP), is created in these high energies nuclei collisions [3]. The models which successfully describe the space-time evolution of QGP fireball are governed by relativistic hydrodynamic models [4–11], which gives information that the shear viscosity to entropy density (η/s) ratio of produced QGP is very small. Also, the experimental data analysis at the RHIC suggests that $\eta/s \approx 0.1$–0.2 [12,13], which is a strong indicator that the produced QGP in these collisions is strongly coupled because for a strongly coupled system η/s is small. For a weakly coupled system, this ratio is large. One of the essential ways to characterize the properties of sQGP is by using hard probes, which are created in the initial stages of these highly energetic collisions, as their production requires a large momentum transfer. One of the promising hard probes is offered by heavy quarks (HQs), mainly charm and a bottom quark, because they do not constitute the bulk constituents of the matter and because of their large mass compared to the temperature scale generated in these ultrarelativistic heavy ion collisions (uRHICs) [14]. HQs travel in the expanding medium as generated after these collisions and interact with the light particles of the medium. However, their number is most likely to be conserved because of their considerable M/T ratio where M is the mass of the HQ and T is the temperature of the medium. Thus, HQs can experience the complete evolution of the QGP, and as they are produced in out of equilibrium, they are expected to retain their memory of interaction with plasma evolution [14–19]. Also, their thermal production and annihilation can be ignored. In a perturbative QCD (pQCD) framework, the thermalization time of the HQ has been estimated and is of the scale of 10–15 fm/c for the charm quark and the scale of 25–30 fm/c for the bottom quark [14,20–22] for the temperature scales required for QGP formed in RHIC and LHC experiments. Nevertheless, since the lifetime of QGP is around 4–5 fm/c at RHIC and 10–12 fm/c at LHC, therefore one should not expect the complete thermalization of HQs in uRHICs. For the small momentum exchange, the multiple scattering of HQ in a thermalized medium can be dealt with as a Brownian motion, and the Boltzmann equation in that approximation can be reduced

*Contact author: sumit@ph.iitr.ac.in
†Contact author: arbp.phy@gmail.com
‡Contact author: nhaque@niser.ac.in
§Contact author: binoy@ph.iitr.ac.in

to the Fokker-Planck equation [14,20,23,24] which constitutes a simplified version of in-medium dynamics. This method has been widely used [20–22,24–30] to study the experimental observables such as nuclear modification factor (R_{AA}) [31–34] and elliptic flow (v_2) [31] for nonphotonic electron spectra.

HQ production has been explored in the perturbative QCD approach up to the next-to-leading order. In the perturbative realm, before the first experimental result, it was anticipated that their interaction with the medium particles could be described using a pQCD technique, which leads to the expectation of small suppression of the final spectra and a small value of the elliptic flow. Nevertheless, experimental results come with a surprise in which the spectrum of nonphotonic electrons coming from the heavy quark decays has been observed in Au-Au collision at $\sqrt{s} = 200$ GeV at the RHIC [31–33]. This result shows a relatively small R_{AA} and a large value of elliptic flow v_2, which clearly indicates that there is a strong correlation between the HQ and medium constituents, which is beyond the pQCD explanations [20,21,35]. This motivates one to go beyond pQCD to tackle the problem in a nonperturbative manner. One of the approaches is to consider the nonperturbative contribution [25] from the quasihadronic bound states with subsequent hadronization from coalescence and fragmentation [36,37]. Another method consists of the hard thermal loop in the pQCD framework to calculate the Debye mass and running coupling [28,38]. This technique includes the nonperturbative contributions through the inclusion of thermal mass $\sim g(T)T$ where the running coupling has been fitted via lattice thermodynamics [39,40]. All these models are built upon the assumption that collisional energy loss serves as the predominant process in the low-momentum range of charm spectra [22,26,41], i.e., $p_T \lesssim (3\text{–}5)m_{\mathrm{HQ}}$. On the other hand, at high p_T, the radiative effects are dominating even though one can not disregard the collisional processes [42–44]. In the low transverse momentum region, the collisional energy loss process dominated because of the effect that the phase space for the in-medium induced gluon radiation is constrained because of HQ mass, i.e., "dead-cone effect" [45,46]. However, now, at LHC experiments, heavy meson spectra can be observed around 30 GeV. At such high p_T, even HQs become ultrarelativistic, and thus radiative energy loss effects become important.

Energetic particles traversing the QCD medium suffer energy loss through the elastic process and gluon bremsstrahlung. The drag and diffusion of HQs cause them to lose their energies in the medium. Much work has been done in the literature to study the energy loss of HQs. HQ energy loss due to hard and soft collision processes has been studied in Refs. [47,48] and for radiative processes in Refs. [46,49–51]. Recently, the soft contribution of the parton energy loss has been studied within a chiral imbalance in Ref. [52]. Many studies have been done recently in the literature to understand the HQ dynamics like HQ potential [53–55], spectral properties [56], and transport coefficients without [44,57,58] and with bulk viscous medium [59,60]. The transport phenomenon has been studied for various other cases like Polyakov loop plasma [61], semi-QGP [62], and memory effects in HQ dynamics [63,64].

One of the other approaches to studying the nonperturbative phenomenon in HQ dynamics can be made by using the Gribov-Zwanziger [65,66] technique. This method improves the infrared dynamics of QCD through a scale of the order of g^2T, which is known as the magnetic scale of the theory. This model deals with the nonperturbative resummation of the theory, having a mass parameter that captures the nonperturbative essence of the theory. For some good reviews, one can look at Refs. [67,68]. This approach has been extended by including the impact of a local composite operator, which consists of a mass term of the order of electric scale $g(T)T$. For more details on this extended Gribov-Zwanziger method, see some of the recent works in Refs. [69–79] and references therein. This extended approach with mass term inclusion in the propagator gives results that are very promising with lattice calculations in the infrared domain, as shown in Ref. [69]. Also, at zero temperature, it has been shown in Refs. [80,81] that this mass term inclusion in the gluon and ghost propagator of the usual Faddeev-Popov quantization is in excellent agreement with lattice results. More details about this can be found in a recent review [82].

Without any mass term, this scheme has been quite successful in describing the QCD thermodynamics when a comparison with lattice simulations was made in Ref. [83]. Also, the other exciting studies which have been done in the recent literature explore quark dispersion relations [84], a connection between Gribov quantization and confinement-deconfinement transition [85], the transport coefficients [86–88], the dilepton production rate being calculated along with quark number susceptibility [89], screening masses of mesons [90], and electromagnetic Debye mass [91], which gives some interesting results of the said observables. In the context of HQ phenomenology, which we are interested in here, the heavy quarkonium potential has been calculated using this method in Refs. [91–93], the collisional energy loss of HQs has been estimated in Ref. [94] incorporating the formalism of Wong equations, and the HQ diffusion coefficient using Langevin dynamics has been studied in Ref. [95].

In this work, we explored the finite momentum-dependent [96] drag and diffusion coefficient of HQs using the Gribov gluon propagator. Earlier in the literature, carrying forward the calculation of the drag and diffusion coefficient using the perturbative approaches, there was a need to set some infrared scale to tackle the infrared divergences that arise mainly in t-channel exchange diagrams. The main advantage of this method is that one does

not need any infrared cutoff to put by hand in the matrix element calculation; instead, it comes automatically in the model calculations. Also, as discussed earlier, the ratio of shear viscosity to entropy density, which is an essential observable to quantify the nature of QGP, has been studied earlier using the perturbative methods [97]. It was found that the inclusion of radiative effects in the calculation improves this ratio significantly.

The work is organized as follows. Following this concise Introduction, we will delve into the conventional formalism for calculating the drag and diffusion coefficients of HQs. This will be accomplished using the widely recognized Fokker-Planck method, as detailed in Sec. II. In this section, we will discuss the scattering of $2 \to 2$ collisional process as well as the $2 \to 3$ radiative process. We give the required matrix element calculation, which has been done using the Gribov propagator. Section III focuses on our results for the drag and diffusion coefficient as estimated using the Gribov propagator. A critical observable η/s which is required to understand the nature of the QGP, i.e., whether a medium behaves like a weakly coupled or strongly coupled system, has been plotted using the Gribov propagator. Also, the energy loss of HQs has been discussed within this model for the charm and bottom quarks while traversing the medium. In Sec. IV, we summarize the paper and give further directions.

II. FORMALISM: DRAG AND DIFFUSION COEFFICIENTS

As discussed earlier, the motion of HQs in the QCD medium can be considered as a Brownian motion and is well described by the Fokker-Planck equation [23,24]

$$\frac{\partial f_{\rm HQ}}{\partial t} = \frac{\partial}{\partial p_i}\left[A_i(\boldsymbol{p}) f_{\rm HQ} + \frac{\partial}{\partial p_j}[B_{ij}(\boldsymbol{p}) f_{\rm HQ}]\right], \tag{1}$$

where $f_{\rm HQ}$ represents the HQ momentum distribution in the medium. In this approach, the interaction of HQ with the medium constituent particles, which are light quarks, antiquarks, and gluons, is encoded in the drag and diffusion tensors A_i and B_{ij}, respectively, which naturally arise from the momentum expansion of the collision integral of the Boltzmann transport equation [23]. In the following, we briefly discuss the essential steps to obtain the drag and diffusion tensor of the HQ. For clarity, the collisional and the radiative contributions are discussed in separate subsections.

A. Collisional processes

Let us start with the two-body elastic scattering process, $\mathrm{HQ}(P) + l(Q) \to \mathrm{HQ}(P') + l(Q')$, where l denotes light particles, viz., light quarks, antiquarks, and gluons. Here, the 4-momentum of the HQ and the constituent particle before the collision are represented by $P = (E_p, \boldsymbol{p})$ and $Q = (E_q, \boldsymbol{q})$ respectively. The corresponding 4-momentum after the collision is denoted with primes. Note that, in the case of the HQ, the energy is given by $E_p = (|\boldsymbol{p}|^2 + m_{\rm HQ}^2)^{1/2}$, whereas the light particles are considered to be massless with $E_q = |\boldsymbol{q}|$. The drag and the diffusion tensor that govern the dynamics of the HQ in the QGP medium can be related to the $2 \to 2$ scattering amplitude as [23]

$$\begin{aligned} A_i = & \frac{1}{2E_p}\int \frac{d^3\boldsymbol{q}}{(2\pi)^3 2E_q}\int \frac{d^3\boldsymbol{q}'}{(2\pi)^3 2E_{q'}}\int \frac{d^3\boldsymbol{p}'}{(2\pi)^3 2E_{p'}}\frac{1}{g_{\rm HQ}} \\ & \times \sum |\mathfrak{M}_{2\to 2}|^2 (2\pi)^4 \delta^4(P + Q - P' - Q') f_k(E_q) \\ & \times [1 + a_k f_k(E_{q'})][(\boldsymbol{p} - \boldsymbol{p}')_i] \\ = & \langle\langle (\boldsymbol{p} - \boldsymbol{p}')_i \rangle\rangle, \end{aligned} \tag{2}$$

$$B_{ij} = \frac{1}{2}\langle\langle (\boldsymbol{p} - \boldsymbol{p}')_i (\boldsymbol{p} - \boldsymbol{p}')_j \rangle\rangle. \tag{3}$$

The expressions above indicate that the drag force represents the thermal average of the momentum transfer $(\boldsymbol{p} - \boldsymbol{p}')$ resulting from interactions. On the other hand, momentum diffusion quantifies the average square of the momentum transfer. In these expressions, $g_{\rm HQ}$ represents the statistical degeneracy factor of the HQ, and the subscript k denotes the particle species in the medium. The quantity $a_k = 1, -1$ represents, respectively, the near-equilibrium Bose-Einstein and the Fermi-Dirac distributions denoted in general as f_k. The delta function enforces the energy-momentum conservation. The computation of the matrix amplitude $\mathfrak{M}_{2\to 2}$ for the allowed $2 \to 2$ scattering processes will be discussed in the following subsection. It should be noted that the drag force depends only on HQ momentum. Thus, one can decompose it as

$$A_i = p_i A(p^2), \qquad A = \langle\langle 1 \rangle\rangle - \frac{\langle\langle \boldsymbol{p}\cdot\boldsymbol{p}' \rangle\rangle}{p^2}, \tag{4}$$

where $p^2 = |\boldsymbol{p}|^2$ and A is the drag coefficient of HQ. Similarly, one can decompose the diffusion tensor B_{ij} in terms of transverse and longitudinal components with respect to HQ momentum as

$$B_{ij} = \left(\delta_{ij} - \frac{p_i p_j}{p^2}\right) B_0(p^2) + \frac{p_i p_j}{p^2} B_1(p^2), \tag{5}$$

where the transverse diffusion coefficient B_0 and longitudinal diffusion coefficient B_1 take the following forms:

$$B_0 = \frac{1}{4}\left[\langle\langle p'^2 \rangle\rangle - \frac{\langle\langle (\boldsymbol{p}'\cdot\boldsymbol{p})^2 \rangle\rangle}{p^2}\right], \tag{6}$$

$$B_1 = \frac{1}{2}\left[\frac{\langle\langle (\boldsymbol{p}'\cdot\boldsymbol{p})^2 \rangle\rangle}{p^2} - 2\langle\langle \boldsymbol{p}'\cdot\boldsymbol{p} \rangle\rangle + p^2 \langle\langle 1 \rangle\rangle\right]. \tag{7}$$

One can study the kinematics of the $2 \to 2$ process in the center-of-momentum (COM) frame for simplification. The average of a generic function $F(\boldsymbol{p})$ in the COM frame can be written as [23,98]

$$\langle\langle F(\boldsymbol{p})\rangle\rangle = \frac{1}{(512\pi^4)E_p g_{\rm HQ}}\int_0^\infty q\,dq\left(\frac{s-m_{\rm HQ}^2}{s}\right)f_k(E_q) \times \int_0^\pi d\chi\,\sin\chi\int_0^\pi d\theta_{\rm cm}\sin\theta_{\rm cm}\sum|\mathfrak{M}_{2\to2}|^2 \times \int_0^{2\pi} d\phi_{\rm cm}[1+a_k f_k(E_{q'})]F(\boldsymbol{p}), \tag{8}$$

where χ quantifies the angle between the incident HQ and the medium constituent particles in the laboratory frame, while $\theta_{\rm cm}$ and $\phi_{\rm cm}$ are, respectively, the zenith and azimuthal angles in the COM frame. The Mandelstam variables s, t, and u are defined as follows:

$$\begin{aligned} s &= (P+Q)^2 = (E_p+E_q)^2-(p^2+q^2+2pq\cos\chi),\\ t &= (P'-P)^2 = 2p_{\rm cm}^2(\cos\theta_{\rm cm}-1),\\ u &= (P'-Q)^2 = 2m_{\rm HQ}^2 - s - t. \end{aligned} \tag{9}$$

Here, $p_{\rm cm} = |\boldsymbol{p}_{\rm cm}|$ is the magnitude of the initial momentum of the HQ in the COM frame. The other quantity required in order to obtain the drag and diffusion coefficients is $(\boldsymbol{p}\cdot\boldsymbol{p}')$. In order to find this quantity, we need the Lorentz transformation that relates the laboratory frame and the COM frame via the relation $\boldsymbol{p}' = \gamma_{\rm cm}(\hat{\boldsymbol{p}}'_{\rm cm} + \boldsymbol{v}_{\rm cm}\hat{E}'_{\rm cm})$, where $\gamma_{\rm cm} = (E_p+E_q)/\sqrt{s}$ and the velocity in the COM is given by $\boldsymbol{v}_{\rm cm} = (\boldsymbol{p}+\boldsymbol{q})/(E_p+E_q)$. Now, the energy conservation dictates $\hat{p}'^2_{\rm cm} = \hat{p}^2_{\rm cm}$. In the COM frame, $\hat{\boldsymbol{p}}'_{\rm cm}$ can be decomposed as $\hat{\boldsymbol{p}}'_{\rm cm} = \hat{p}_{\rm cm}(\cos\theta_{\rm cm}\hat{\boldsymbol{x}}_{\rm cm} + \sin\theta_{\rm cm}\sin\phi_{\rm cm}\hat{\boldsymbol{y}}_{\rm cm} + \sin\theta_{\rm cm}\cos\phi_{\rm cm}\hat{\boldsymbol{z}}_{\rm cm})$, where $\hat{p}_{\rm cm} = (s-m_{\rm HQ}^2)/(2\sqrt{s})$ is the momentum and $\hat{E}_{\rm cm} = (\hat{p}^2_{\rm cm}+m^2_{\rm HQ})^{1/2}$ is the energy of the HQ in the COM frame. The axes $\hat{\boldsymbol{x}}_{\rm cm}, \hat{\boldsymbol{y}}_{\rm cm}$, and $\hat{\boldsymbol{z}}_{\rm cm}$ are defined in Ref. [23].

Utilizing the above definitions, one can obtain

$$\boldsymbol{p}\cdot\boldsymbol{p}' = E_pE'_p - \hat{E}^2_{\rm cm} + \hat{p}^2_{\rm cm}\cos\theta_{\rm cm}. \tag{10}$$

B. Matrix elements for $2 \to 2$ processes

The leading order Feynman diagrams for $2 \to 2$ processes are shown in Fig. 1. There are three topologically distinct diagrams contributing to quark-gluon scattering shown in Figs. 1(a)–1(c) one diagram for quark-quark or quarkantiquark scattering shown in Fig. 1(d) [99]. Note that each of the diagrams shown in Figs. 1(a) and 1(d) possesses a gluon propagator, which in the present work has been replaced with the Gribov-modified gluon propagator. The modified gluon propagator in the Landau gauge is given as [83]

$$D^{ab}_{\mu\nu}(P) = \delta^{ab}\left(\delta_{\mu\nu} - \frac{P_\mu P_\nu}{P^2}\right)\frac{P^2}{P^4+\gamma_{\rm G}^4}, \tag{11}$$

where $\gamma_{\rm G}$ is the Gribov mass parameter which is generally derived from the one-loop or two-loop gap equation [79]. The matrix elements for the diagrams shown in Fig. 1, using the Gribov propagator, are given by

$$\begin{aligned} \mathfrak{M}_{\rm (a)} &= -g^2\varepsilon_\mu(2)\varepsilon^*_\nu(4)f_{abc}[g^{\mu\nu}(-Q-Q')^\rho + g^{\nu\rho}(2Q'-Q)^\mu + g^{\rho\mu}(2Q-Q')^\nu]\frac{(P'-P)^2}{(P'-P)^4+\gamma_{\rm G}^4}\bar{u}^i(3)\gamma_\rho\lambda_c u^i(1),\\ \mathfrak{M}_{\rm (b)} &= -ig^2\varepsilon_\mu(2)\varepsilon^*_\nu(4)\bar{u}^i(3)\gamma^\mu\lambda_a\frac{\not{P}+\not{Q}+m_{\rm HQ}}{(P+Q)^2-m^2_{\rm HQ}}\gamma^\nu\lambda_b u^i(1),\\ \mathfrak{M}_{\rm (c)} &= -ig^2\varepsilon_\mu(2)\varepsilon^*_\nu(4)\bar{u}^i(3)\gamma^\nu\lambda_b\frac{\not{P}'-\not{Q}+m_{\rm HQ}}{(P'-Q)^2-m^2_{\rm HQ}}\gamma^\mu\lambda_a u^i(1),\\ \mathfrak{M}_{\rm (d)} &= ig^2\bar{u}^i(3)\gamma^\mu\lambda_a u^i(1)\frac{(P'-P)^2}{(P'-P)^4+\gamma_{\rm G}^4}\bar{u}^i(4)\gamma_\mu\lambda_a u^i(2). \end{aligned} \tag{12}$$

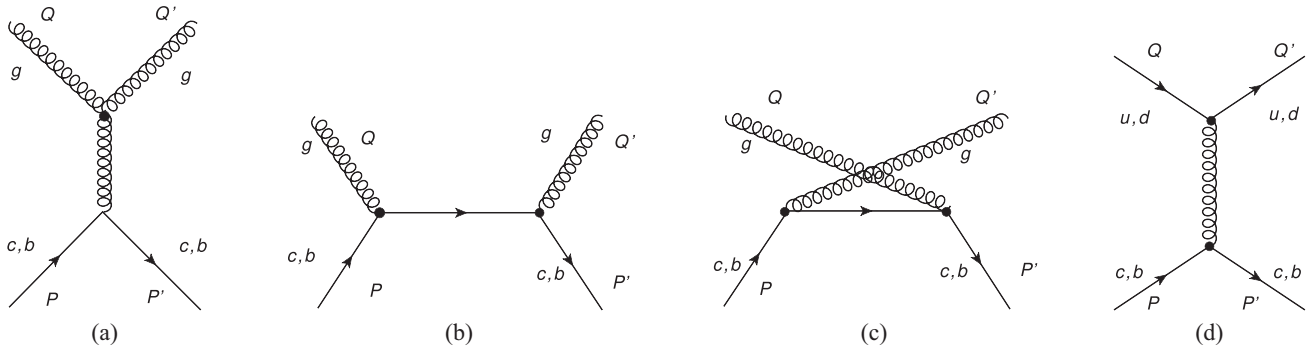

FIG. 1. Feynman diagrams for HQ $2 \to 2$ processes with (a) gluon (t channel), (b) gluon (s channel), (c) gluon (u channel), and (d) light quark/antiquark (t channel).

Here, the abbreviated notations used are $\varepsilon_\mu(1) = \varepsilon_\mu(P,\zeta_P), \varepsilon_\mu(2) = \varepsilon_\mu(Q,\zeta_Q), \varepsilon_\mu(3) = \varepsilon_\mu(P',\zeta_{P'})$, and $\varepsilon_\mu(4) = \varepsilon_\mu(Q,\zeta_{Q'})$ for gluon polarization vectors; i denotes different flavors; and $u(1) = u(P,s_P)$ denotes quark spinors. The symbols λ_a represent $SU(3)$ matrices normalized by $\mathrm{Tr}(\lambda_a\lambda_b) = \frac{1}{2}\delta_{ab}$, satisfying $[\lambda_a,\lambda_b] = if_{abc}\lambda_c$, and f_{abc} are the structure constants. The summation of squared matrix elements over the initial and final quark spin states transforms the quark spinors into projection operators as per the relation

$$\sum_{s=1,2} u^i_\alpha(P,s)\bar{u}^i_\beta(P,s) = (\not{P} + m^i_{\mathrm{HQ}})_{\alpha\beta}. \tag{13}$$

During summation over gluon polarizations ζ_r where $r = 1, 2, 3, 4$, in order to avoid the contributions from the unphysical states, one can remove the terms containing $\varepsilon_\mu(P,\zeta)P^\mu$. Thus, the amplitude $\mathfrak{M}_{(\mathrm{a})}$ becomes

$$\mathfrak{M}_{(\mathrm{a})} = -g^2\varepsilon_\mu(2)\varepsilon^*_\nu(4)f_{abc}[g^{\mu\nu}(-Q-Q')^\rho + g^{\nu\rho}(2Q')^\mu + g^{\rho\mu}(2Q)^\nu]\frac{(P'-P)^2}{(P'-P)^4+\gamma_{\mathrm{G}}^4}\bar{u}^i(3)\gamma_\rho\lambda_c u^i(1). \tag{14}$$

Now, one can do the trace over the Lorentz indices utilizing the relation

$$\sum_{\zeta=1,2}\varepsilon^*_\mu(P,\zeta)\varepsilon_\nu(P,\zeta) = -g_{\mu\nu}. \tag{15}$$

The squared matrix elements can be conveniently written in terms of Mandelstam variables, which satisfy the relation $s+t+u = 2m^2_{\mathrm{HQ}}$. After doing the summation over the spins, polarizations, and color indices, one would get the final expressions as follows:

(i) For the process $\mathrm{HQ}(P) + g(Q) \to \mathrm{HQ}(P') + g(Q')$, one obtains

$$|\mathfrak{M}_{(a)}|^2 = g_{\mathrm{HQ}}g_g\left[32\pi^2\alpha^2\frac{(s-m^2_{\mathrm{HQ}})(m^2_{\mathrm{HQ}}-u)t^2}{(t^2+\gamma_{\mathrm{G}}^4)^2}\right],$$

$$|\mathfrak{M}_{(b)}|^2 = g_{\mathrm{HQ}}g_g\left[\frac{64\pi^2\alpha^2}{9}\frac{(s-m^2_{\mathrm{HQ}})(m^2_{\mathrm{HQ}}-u)+2m^2_{\mathrm{HQ}}(s+m^2_{\mathrm{HQ}})}{(s-m^2_{\mathrm{HQ}})^2}\right],$$

$$|\mathfrak{M}_{(c)}|^2 = g_{\mathrm{HQ}}g_g\left[\frac{64\pi^2\alpha^2}{9}\frac{(s-m^2_{\mathrm{HQ}})(m^2_{\mathrm{HQ}}-u)+2m^2_{\mathrm{HQ}}(m^2_{\mathrm{HQ}}+u)}{(m^2_{\mathrm{HQ}}-u)^2}\right],$$

$$\mathfrak{M}_{(a)}\mathfrak{M}^*_{(b)} = \mathfrak{M}^*_{(b)}\mathfrak{M}_{(a)} = g_{\mathrm{HQ}}g_g\left[8\pi^2\alpha^2\frac{(s-m^2_{\mathrm{HQ}})(m^2_{\mathrm{HQ}}-u)+m^2_{\mathrm{HQ}}(s-u)}{\left(\frac{t^2+\gamma_{\mathrm{G}}^4}{t}\right)(s-m^2_{\mathrm{HQ}})}\right],$$

$$\mathfrak{M}_{(a)}\mathfrak{M}^*_{(c)} = \mathfrak{M}^*_{(c)}\mathfrak{M}_{(a)} = g_{\mathrm{HQ}}g_g\left[8\pi^2\alpha^2\frac{(s-m^2_{\mathrm{HQ}})(m^2_{\mathrm{HQ}}-u)-m^2_{\mathrm{HQ}}(s-u)}{\left(\frac{t^2+\gamma_{\mathrm{G}}^4}{t}\right)(m^2_{\mathrm{HQ}}-u)}\right],$$

$$\mathfrak{M}_{(b)}\mathfrak{M}^*_{(c)} = \mathfrak{M}^*_{(b)}\mathfrak{M}_{(c)} = g_{\mathrm{HQ}}g_g\left[\frac{8\pi^2\alpha^2}{9}\frac{m^2_{\mathrm{HQ}}(4m^2_{\mathrm{HQ}}-t)}{(s-m^2_{\mathrm{HQ}})(m^2_{\mathrm{HQ}}-u)}\right],$$

$$|\mathfrak{M}_{(i)}|^2 = |\mathfrak{M}_{(a)}|^2 + |\mathfrak{M}_{(b)}|^2 + |\mathfrak{M}_{(c)}|^2 + 2\mathcal{R}e\left\{\mathfrak{M}_{(a)}\mathfrak{M}^*_{(b)}\right\} + 2\mathcal{R}e\left\{\mathfrak{M}_{(b)}\mathfrak{M}^*_{(c)}\right\} + 2\mathcal{R}e\left\{\mathfrak{M}_{(a)}\mathfrak{M}^*_{(c)}\right\}. \tag{16}$$

(ii) For the process $\mathrm{HQ}(P) + lq(Q)/l\bar{q}(Q) \to \mathrm{HQ}(P') + lq(Q')/l\bar{q}(Q')$, one obtains

$$|\mathfrak{M}_{(d)}|^2 = g_{\mathrm{HQ}}g_{lq/l\bar{q}}\left[\frac{64\pi^2\alpha^2}{9}\frac{\left((s-m^2_{\mathrm{HQ}})^2+(m^2_{\mathrm{HQ}}-u)^2+2m^2_{\mathrm{HQ}}\left(\frac{t^2+\gamma_{\mathrm{G}}^4}{t}\right)\right)t^2}{(t^2+\gamma_{\mathrm{G}}^4)^2}\right]. \tag{17}$$

Here, $g_{\mathrm{HQ}} = N_s \times N_c$, $g_g = N_s \times (N_c^2-1)$, and $g_{lq/l\bar{q}} = N_s \times N_c \times N_f$ are the degeneracy factor for HQ, gluon, and light quark, respectively, where $N_s = 2$, $N_f = 3$, and $N_c = 3$ have been used.

C. Radiative process

In general, the transport coefficient can be written [97] as

$$\mathrm{X(p)} = \int \text{phase space} \times \text{interaction} \times \text{transport part}. \quad (18)$$

Equation (18) can be used in order to study the radiative contribution of the drag and diffusion coefficient by replacing the two-body phase space and invariant amplitude with their three-body counterparts, keeping the transport part the same [97]. Let us consider the $2 \to 3$ inelastic process $\mathrm{HQ}(P) + l(Q) \to \mathrm{HQ}(P') + l(Q') + g(K')$, where $K' = (E_{k'}, \boldsymbol{k}'_\perp, k'_z)$ is the 4-momentum of the emitted soft gluon by HQ in the final state. The general expression for the thermal averaged $\langle\langle F(\boldsymbol{p})\rangle\rangle$ for $2 \to 3$ process is given by [97]

$$\begin{aligned}\langle\langle F(\boldsymbol{p})\rangle\rangle_{\mathrm{rad}} = &\frac{1}{2E_p g_{\mathrm{HQ}}}\int\frac{d^3\boldsymbol{q}}{(2\pi)^3E_q}\int\frac{d^3\boldsymbol{q}'}{(2\pi)^3E_{q'}}\int\frac{d^3\boldsymbol{p}'}{(2\pi)^3E_{p'}}\\ &\times\int\frac{d^3\boldsymbol{k}'}{(2\pi)^3E_{k'}}\sum|\mathfrak{M}_{2\to3}|^2 f_k(E_q)(1\pm f_k(E_{q'}))\\ &\times(1+f_g(E_{k'}))\theta_1(E_p-E_{k'})\theta_2(\tau-\tau_F)\\ &\times F(\boldsymbol{p})(2\pi)^4\delta^{(4)}(P+Q-P'-Q'-K'), \quad (19)\end{aligned}$$

where τ is the scattering time of HQ with the medium constituents and τ_F is the formation time of gluons. The theta function $\theta_1(E_p - E_{k'})$ in Eq. (19) imposes the constraints on the process that the emitted gluon energy should be less than the initial energy of HQ, whereas, the second theta function $\theta_2(\tau - \tau_F)$ makes sure that the formation time of the gluon should be less than the scattering time of HQs with medium constituents that accounts for the Landau-Pomerancguk-Migdal effect [100–102]. Also, $f_g(E_{k'}) = 1/[\exp(\beta E_{k'}) - 1]$ is the distribution of the emitted gluon where $\beta = 1/T$, i.e., the gluons in Figs. 1 and 2 are in thermally equilibrated state. The term $|\mathfrak{M}_{2\to3}|^2$ denotes the matrix element squared for the $2 \to 3$ radiative process as depicted in Fig. 2. It can be expressed in terms of the matrix element of the collision process multiplied by the probability for soft gluon emission [103] as follows,

$$|\mathfrak{M}_{2\to3}|^2 = |\mathfrak{M}_{2\to2}|^2 \times \frac{12g_s^2}{k_\perp'^2}\left(1+\frac{m_{\mathrm{HQ}}^2}{s}e^{2\eta}\right)^{-2}, \quad (20)$$

where g_s is the strong running coupling defined at one loop as

$$g_s^2(T) = 4\pi\alpha_s = \frac{24\pi^2}{11N_c - 2N_f}\frac{1}{\ln(2\pi T/\Lambda_{\overline{\mathrm{MS}}})} \quad (21)$$

having scale $\Lambda_{\overline{\mathrm{MS}}} = 0.176$ GeV [104] for $N_f = 3$, where η is the rapidity of the emitted gluon and $(1+\frac{m_{\mathrm{HQ}}^2}{s}e^{2\eta})^{-2}$ is the suppression factor for the HQ due to the dead-cone factor [45,103]. From Eq. (19), we have

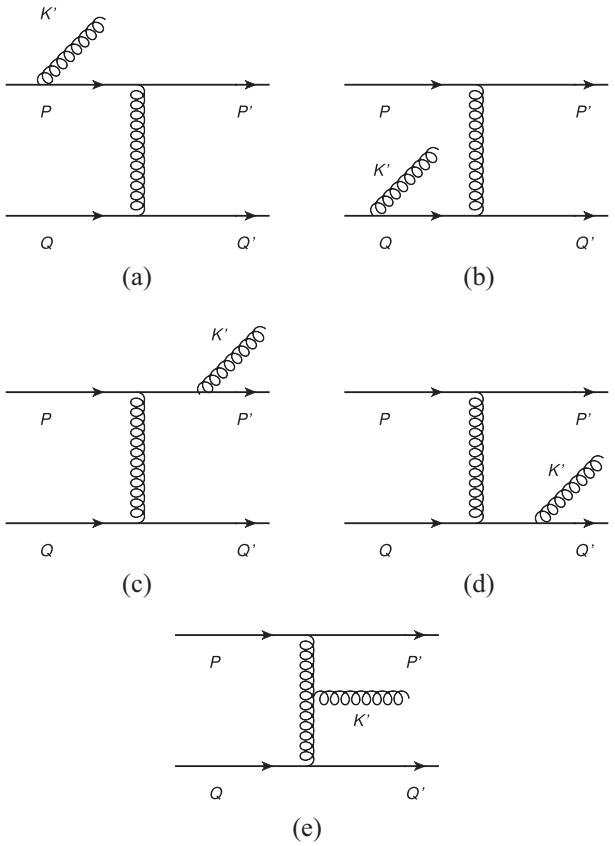

FIG. 2. Feynman diagrams for process $\mathrm{HQ}(P) + l(Q) \to \mathrm{HQ}(P') + l(Q') + g(K')$, showing an inelastic scattering of HQ with light quark and a soft gluon emission.

$$\langle\langle F(\boldsymbol{p})\rangle\rangle_{\mathrm{rad}} = \langle\langle F(\boldsymbol{p})\rangle\rangle_{\mathrm{coll}} \times \mathfrak{F}(\boldsymbol{p}), \quad (22)$$

where $\mathfrak{F}(\boldsymbol{p})$ is given by

$$\begin{aligned}\mathfrak{F}(\boldsymbol{p}) = &\int\frac{d^3k'}{(2\pi)^3 2E_{k'}}\frac{12g_s^2}{k_\perp'^2}\left(1+\frac{m_{\mathrm{HQ}}^2}{s}e^{2\eta}\right)^{-2}\\ &\times(1+f_g(E_{k'}))\theta_1(E_p-E_{k'})\theta_2(\tau-\tau_F). \quad (23)\end{aligned}$$

In the limit of soft gluon emission ($\theta_{k'} \to 0$), one will get $(1+\frac{m_{\mathrm{HQ}}^2}{s}e^{2\eta})^{-2} \approx (1+\frac{4m_{\mathrm{HQ}}^2}{s\theta_{k'}^2})^{-2}$, where $\theta_{k'}$ is the angle between the radiated soft gluon and the HQ which can be related to the rapidity parameter through the relation $\eta = -\ln[\tan(\theta_{k'}/2)]$. In order to simplify Eq. (23), one can convert emitted gluon 4-momentum in terms of the rapidity variable as

$$E_{k'} = k'_\perp \cosh\eta, \qquad k'_z = k'_\perp \sinh\eta, \quad (24)$$

with $d^3k' = d^2k'_\perp dk'_z = 2\pi k'^2_\perp dk'_\perp \cosh\eta d\eta$. The interaction time τ is related to the interaction rate $\Gamma = 2.26\alpha_s T$ [59], and the $\theta_2(\tau - \tau_F)$ impose the constraint

$$\tau = \Gamma^{-1} > \tau_F = \frac{\cosh\eta}{k'_\perp}, \tag{25}$$

which shows that $k'_\perp > \Gamma\cosh\eta = (k'_\perp)_{\min}$. Further, from the other theta function $\theta_1(E_p - E_{k'})$, we have

$$E_p > E_{k'} = k'_\perp \cosh\eta, \qquad (k'_\perp)_{\max} = \frac{E_p}{\cosh\eta}. \tag{26}$$

Also, the Bose enhancement factor for the emitted gluon in the limiting case ($E_{k'} \ll T$) can be written as

$$1 + f_g(E_{k'}) = \frac{T}{k'_\perp \cosh\eta}. \tag{27}$$

Thus, the integral $\mathfrak{I}(\boldsymbol{p})$ becomes

$$\mathfrak{I}(\boldsymbol{p}) = \frac{3}{2\pi^2} g_s^2 T \int_{\Gamma\cosh\eta}^{E_p/\cosh\eta} dk'_\perp \int_{-\eta_1}^{\eta_1} d\eta \times \left(1 + \frac{m_{\rm HQ}^2}{s} e^{2\eta}\right)^{-2} \frac{1}{k'_\perp \cosh\eta}, \tag{28}$$

where rapidity integration limits are decided based on the pseudorapidity coverage of the detector accordingly. In the next section, we have used the value of $\eta_1 = 20$ for practical calculations.

III. RESULTS AND DISCUSSION

In order to do a numerical evaluation of drag and diffusion coefficients, first, we must fix the Gribov mass parameter $\gamma_{\rm G}$ appearing in the Gribov propagator. To do so, the authors of Ref. [88] have done the matching of temperature-dependent scaled trace anomaly results of lattice [105] with the equilibrium thermodynamic quantities. In Fig. 3, we show the scaled Gribov mass parameter variation $\gamma_{\rm G}/T$ with temperature T. This dependence of $\gamma_{\rm G}$ will be used in the estimation of other quantities evaluated further. Now, we will present our numerical results for the transport coefficient, namely, drag and diffusion for elastic and inelastic processes, the specific shear viscosity of the QGP medium, and the estimation of collisional and radiative energy loss in the separate subsections.

A. Drag and diffusion coefficient for collisional and radiative processes

In Fig. 4(a), the temperature dependence of the drag coefficient has been shown at $p = 5$ GeV. Here, we have taken the charm quark mass 1.3 GeV. The contributions from both processes have been shown as these processes occur independently in the thermal medium. Figure 4(a) shows that the collisional process contributes more at the low temperature than the radiative one. However, as the temperature increases, the radiative process starts dominating, indicating that inelastic processes are more important at LHC energies than RHIC energy within this model calculations. As the temperature increases, the total contribution to the drag coefficient increases compared to the elastic process. Qualitatively, the drag coefficient has a similar nature within this modeling compared to earlier perturbative results [97]. However, the overall magnitude of both processes is higher after a $T = 0.4$ GeV and lower before $T = 0.4$ GeV, which can be inferred from the nonperturbative nature of the Gribov propagator. As the system with the Gribov gluon propagator is strongly interacting, the HQs feel a strong drag force compared to the weakly interacting matter in the high-temperature domain, while at lower temperature, the HQ drag coefficient is less compared to earlier perturbative estimation. In other words, one would expect a larger drag coefficient in Gribov plasma for large temperatures and a lower drag coefficient for lower temperatures. Thus, the overall magnitude of the drag coefficient for collisional and radiative processes is higher in the high-temperature domain via the Gribov-Zwanziger approach than it was with earlier perturbative results. In Fig. 4(b), the drag coefficient of HQ has been plotted with its momentum for a temperature $T = 0.525$ GeV. It has been observed that after a momentum of 5 GeV, the radiative contribution dominates in the medium despite the dead-cone effect.

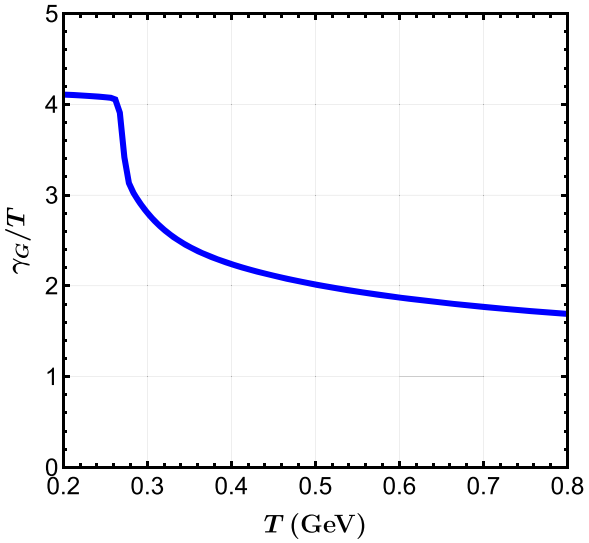

FIG. 3. Temperature dependence of the scaled Gribov mass parameter obtained by matching the thermodynamics of the quasiparticle approach with the pure gauge lattice data [105].

In Figs. 5(a) and 6(a), the variation of the transverse and longitudinal diffusion coefficient of the charm quark is shown with respect to temperature. Similar to the drag coefficient, the radiative effects start dominating for the high-temperature range around $T = 0.6$ GeV. The transverse and the longitudinal diffusion coefficients have a

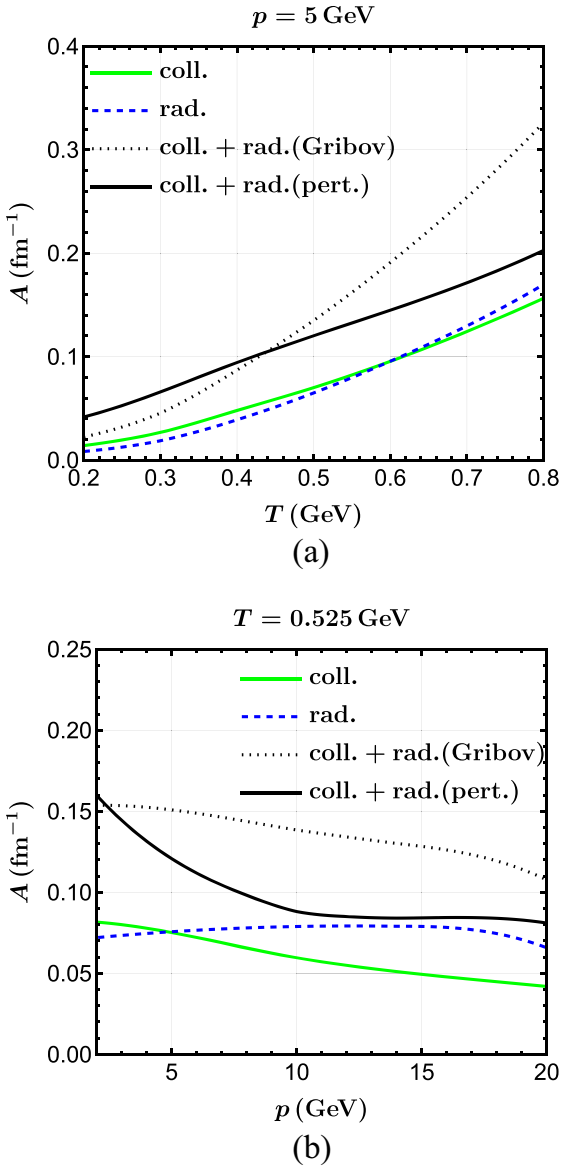

FIG. 4. Variation of charm quark drag coefficient with temperature and momentum at (a) $p = 5$ GeV and (b) $T = 0.525$ GeV, respectively. where "coll." stands for collisional processes and "rad." stands for radiative processes. The same abbreviations have been used for the rest of the Figures.

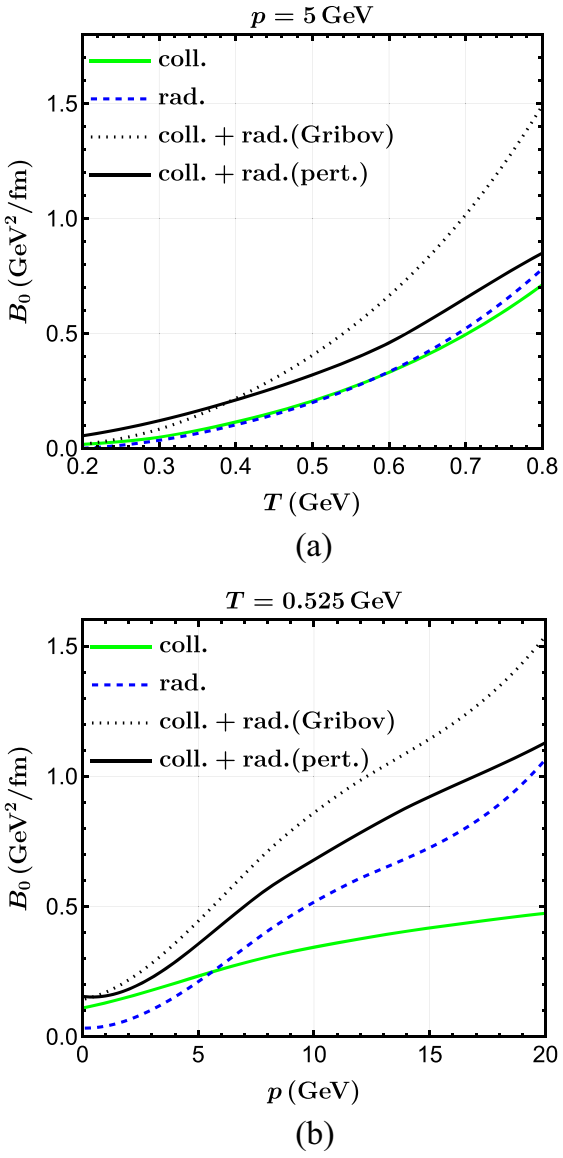

FIG. 5. Variation of charm quark transverse diffusion coefficient with temperature and momentum at (a) $p = 5$ GeV and (b) $T = 0.525$ GeV, respectively.

smaller magnitude before $T \sim 0.45$ GeV and a larger magnitude after $T \sim 0.45$ GeV compared to earlier perturbative results [97], pertaining to the more nonperturbative nature. Similarly, Figs. 5(b) and 6(b) shows the transverse and longitudinal diffusion coefficient variation with the charm momentum at $T = 0.525$ MeV. The variation with the momentum p for the transverse diffusion is smaller than the longitudinal diffusion coefficient. Although the nature of the diffusion coefficient variation differs from the drag coefficient, the radiative effects dominations after $p = 5$ GeV are clearly evident, showing the importance of radiative effects at high momenta.

A similar analysis of drag and diffusion coefficients can be done for bottom quarks having mass approximately as 4.2 GeV easily. We report that for the bottom quarks, the drag coefficient magnitudes decrease compared to the charm quark drag coefficient magnitude because of the greater mass of the bottom quark compared to the charm quark. Similar behavior is also observed for the transverse and longitudinal diffusion coefficients as well.

B. Shear viscosity to entropy density ratio (η/s) of QGP

In this subsection, we estimate the shear viscosity to entropy density ratio by using the Gribov propagator, which enters the interaction part of the diffusion coefficient.

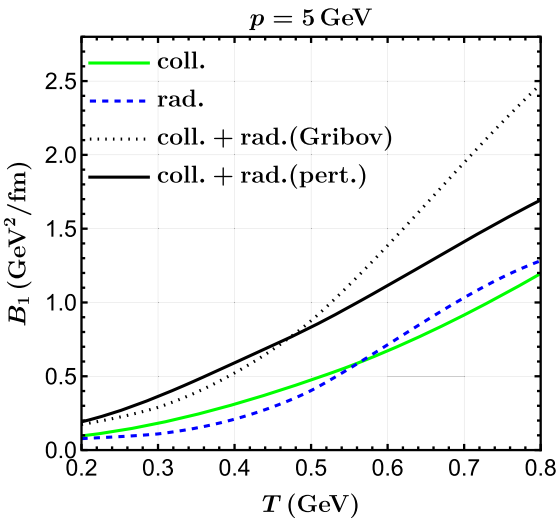

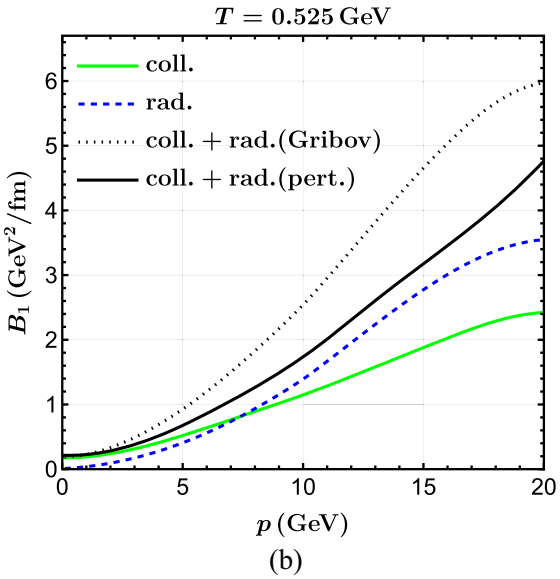

FIG. 6. Variation of charm quark longitudinal diffusion coefficient with temperature and momentum at (a) $p = 5$ GeV and (b) $T = 0.525$ GeV, respectively.

The transverse momentum diffusion coefficient B_0 can be written as

$$B_0 = \frac{1}{2}\left(\delta_{ij} - \frac{p_i p_j}{p^2}\right) B_{ij}. \tag{29}$$

By using Eq. (3) and putting $(p' - p)_i = k_i$,

$$B_0 = \frac{1}{4}\left\langle\!\!\left\langle \left(k^2 - \frac{(\boldsymbol{p}\cdot\boldsymbol{k})^2}{p^2}\right)\right\rangle\!\!\right\rangle. \tag{30}$$

If HQ momentum is considered in the $\hat{z}$ direction, then

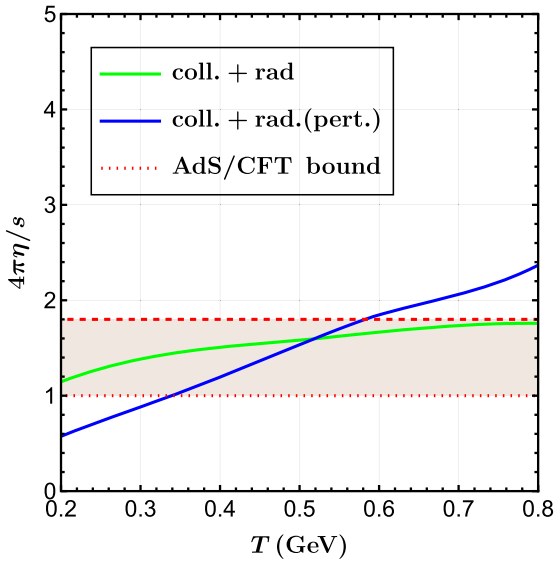

FIG. 7. The value of $4\pi\eta/s$ for a charm quark with momentum $\langle p_z \rangle = 5$ GeV propagating in QGP medium of temperature T.

$$B_0 = \frac{1}{4}\langle\!\langle k_\perp^2 \rangle\!\rangle = \frac{1}{4}\hat{q}, \tag{31}$$

where $\hat{q}$ is the jet quenching parameter, which is also an important quantity for the characterization of QGP. Recently, the relation between these two parameters, namely, specific shear viscosity η/s and dimensionless quenching parameter $\hat{q}/T^3$, has been calculated up to next-to-leading order in terms of coupling constant using perturbative QCD approach in Ref. [106]. Thus, we estimated η/s of QGP using the following expression:

$$\frac{\eta}{s} = 1.63\frac{T^3}{\hat{q}}. \tag{32}$$

Thus,

$$4\pi\frac{\eta}{s} = 1.63\pi\frac{T^3}{B_0}. \tag{33}$$

In Fig. 7, we plotted $4\pi\eta/s$ with respect to temperature T within these model calculations. We compared it with the standard Kovtun-Son-Starinet (KSS) bound having values of $4\pi\eta/s = 1.0$–1.8 as obtained in Ref. [107] as well as with the earlier perturbative result obtained in Ref. [97]. The obtained results show that the value of $4\pi\eta/s$ comes strictly within the AdS/CFT bound after the inclusion of radiative processes, which further improves the earlier perturbative results and shows good agreement with the experimental values [12,13]. For the earlier perturbative results, the Debye mass (m_D) acts as an infrared regulator, and the value of $m_D = \sqrt{3/2}g_s T$ is used in Figs. 4–7 for the perurbative result comparison with Gribov-Zwanziger (GZ) estimations. Thus, one can infer that the Gribov-Zwanziger technique improves the perturbative results in

the low-temperature domain as well as in the high-temperature domain, as can be observed in Fig. 7.

C. Collisional and radiative energy loss

The differential energy loss of the HQ is related to the drag coefficient [24] and can be expressed as

$$-\frac{dE}{dx} = A(p^2, T)p. \tag{34}$$

In Fig. 8, we have plotted the energy loss of HQs with respect to their momentum p, showing collisional and radiative contributions independently at RHIC and LHC energies. In Fig. 8(a), the energy loss at RHIC energy ($T = 0.36$ GeV) for charm (solid lines) and bottom (dotted lines) quarks are shown. Similarly, Fig. 8(b) has been plotted for temperature $T = 0.48$ GeV, i.e., at LHC energy. As expected, energy loss for the bottom quark is less compared to the charm quark because of more drag offered to the bottom quark in the medium due to its large mass. Due to restricted phase space, the collisional processes dominate in the initial momentum range around 5 GeV. However, after that, the radiative process dominates the collisional one for charm quark at both energies at the LHC and RHIC. In the case of the bottom quark, the collisional process contribution dominates in the whole momentum range at the RHIC. At the same time, this nature continues at LHC energy until ~15 GeV; then, the radiative process dominates. This suppression in the radiative energy loss in the case of the bottom quark in comparison to the charm quark can be accounted for because of the dead-cone factor, which prohibits the HQ from radiating gluon at a small angle. Thus, the dead-cone angle will be large for the higher mass, and the probability of energy loss due to radiation will be less.

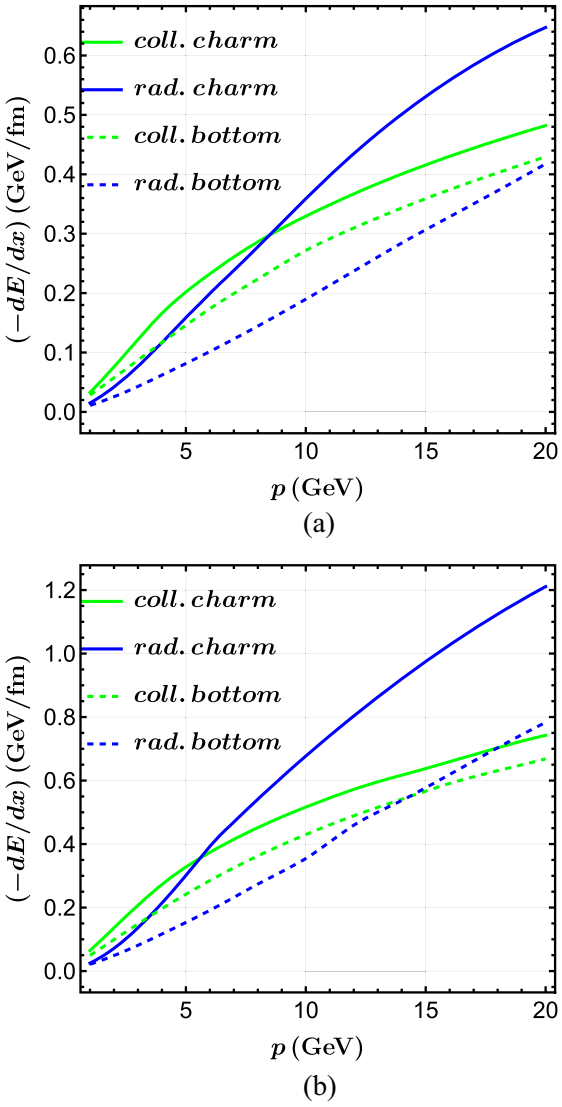

FIG. 8. Momentum variation of elastic and radiative energy loss of the HQs in the medium for the RHIC energy at $T = 360$ MeV (upper panel) and the LHC energy at $T = 480$ MeV (lower panel). Solid lines are for charm quarks, while dotted ones are for bottom quarks.

IV. CONCLUSION

In this work, we have investigated the momentum and temperature dependence of the drag and diffusion coefficient of HQs propagating in the QGP medium. These transport coefficients play a pivotal role in the HQ phenomenology as they essentially govern the dynamics of the HQs in the Fokker-Planck approach. In the present work, our primary focus has been to incorporate the nonperturbative effects in the estimation of drag and diffusion coefficients, especially in the temperature regime close to the crossover. For this purpose, we take recourse to the Gribov-Zwanziger method. In this framework, the gluon propagators present in the scattering amplitudes have been replaced by the Gribov-modified propagators. It should be noted here that it has been a standard practice to include the Debye mass [$m_D \sim g(T)T$] as an infrared regulator in the t-channel matrix amplitude in order to circumvent the infrared divergence. However, in the present work, the mass scale in the modified gluon propagator arises naturally within the model framework, resulting in a finite t-channel contribution. The temperature dependence of the mass scale has been extracted by matching the thermodynamics of the Gribov plasma with the pure gauge lattice results. Once the temperature dependence has been fixed, we incorporate this modified gluon propagator in the collisional and radiative contributions to obtain the momentum and temperature dependences of the drag and diffusion coefficient, which show a significant increment compared to earlier perturbative estimations. Moreover, we find that the estimation of the specific shear viscosity using the Gribov method is in better agreement with the AdS/CFT calculations. Finally, we have investigated the collisional and radiative energy loss of the charm and bottom quark traversing through the medium. We find that the energy loss

in both cases is higher in magnitude compared to the earlier perturbative estimations.

It should be mentioned here that the Gribov framework presented in this work is a simplistic approach to incorporate the nonperturbative effects relevant near the phenomenologically accessible temperature regime. Nevertheless, the present study serves as an important first step toward estimating the impact of Gribov-like approaches on the HQ dynamics and encourages one to study further different experimental observables like nuclear modification factor R_{AA} [94], elliptic flow v_2, and other transport properties of the medium [86–88,108,109] within this framework. An interesting future direction in this regard would be to incorporate the dissipative effects in the estimation of drag and diffusion tensor of the HQ [98,110–113]. Also, the nontrivial backgrounds like the strong external magnetic field may have a significant impact [114–116] on the transport properties of the Gribov modified plasma medium. We relegate such studies for future explorations.

ACKNOWLEDGMENTS

We would like to thank Raktim Abir for the helpful discussion. N. H. is supported in part by the SERB-Mathematical Research Impact Centric Support (MATRICS) under Grant No. MTR/2021/000939.

[1] E. V. Shuryak, What RHIC experiments and theory tell us about properties of quark-gluon plasma?, Nucl. Phys. **A750**, 64 (2005).
[2] B. V. Jacak and B. Muller, The exploration of hot nuclear matter, Science **337**, 310 (2012).
[3] M. Gyulassy and L. McLerran, New forms of QCD matter discovered at RHIC, Nucl. Phys. **A750**, 30 (2005).
[4] D. Teaney, J. Lauret, and E. V. Shuryak, Flow at the SPS and RHIC as a quark gluon plasma signature, Phys. Rev. Lett. **86**, 4783 (2001).
[5] P. Huovinen, P. F. Kolb, U. W. Heinz, P. V. Ruuskanen, and S. A. Voloshin, Radial and elliptic flow at RHIC: Further predictions, Phys. Lett. B **503**, 58 (2001).
[6] C. Nonaka and S. A. Bass, Space-time evolution of bulk QCD matter, Phys. Rev. C **75**, 014902 (2007).
[7] H. Song and U. W. Heinz, Suppression of elliptic flow in a minimally viscous quark-gluon plasma, Phys. Lett. B **658**, 279 (2008).
[8] M. Luzum and P. Romatschke, Conformal relativistic viscous hydrodynamics: Applications to RHIC results at $\sqrt{s} = 200$ GeV, Phys. Rev. C **78**, 034915 (2008); **79**, 039903(E) (2009).
[9] Z. Qiu, C. Shen, and U. Heinz, Hydrodynamic elliptic and triangular flow in Pb-Pb collisions at $\sqrt{s} = 2.76$ ATeV, Phys. Lett. B **707**, 151 (2012).
[10] L. Pang, Q. Wang, and X. N. Wang, Effect of longitudinal fluctuation in event-by-event $(3+1)$D hydrodynamics, Nucl. Phys. **A904–905**, 811c (2013).
[11] C. Gale, S. Jeon, B. Schenke, P. Tribedy, and R. Venugopalan, Event-by-event anisotropic flow in heavy-ion collisions from combined Yang-Mills and viscous fluid dynamics, Phys. Rev. Lett. **110**, 012302 (2013).
[12] J. E. Bernhard, J. S. Moreland, and S. A. Bass, Bayesian estimation of the specific shear and bulk viscosity of quark–gluon plasma, Nat. Phys. **15**, 1113 (2019).
[13] D. Everett *et al.* (JETSCAPE Collaboration), Multisystem Bayesian constraints on the transport coefficients of QCD matter, Phys. Rev. C **103**, 054904 (2021).
[14] R. Rapp and H. van Hees, Heavy quarks in the quark-gluon plasma, arXiv:0903.1096.
[15] A. Andronic, F. Arleo, R. Arnaldi, A. Beraudo, E. Bruna, D. Caffarri, Z. C. del Valle, J. G. Contreras, T. Dahms, A. Dainese *et al.*, Heavy-flavour and quarkonium production in the LHC era: From proton–proton to heavy-ion collisions, Eur. Phys. J. C **76**, 107 (2016).
[16] F. Prino and R. Rapp, Open heavy flavor in QCD matter and in nuclear collisions, J. Phys. G **43**, 093002 (2016).
[17] G. Aarts, J. Aichelin, C. Allton, R. Arnaldi, S. A. Bass, C. Bedda, N. Brambilla, E. Bratkovskaya, P. Braun-Munzinger, G. E. Bruno *et al.*, Heavy-flavor production and medium properties in high-energy nuclear collisions—What next?, Eur. Phys. J. A **53**, 93 (2017).
[18] V. Greco, Heavy flavor production, flow and energy loss, Nucl. Phys. **A967**, 200 (2017).
[19] J. Zhao, K. Zhou, S. Chen, and P. Zhuang, Heavy flavors under extreme conditions in high energy nuclear collisions, Prog. Part. Nucl. Phys. **114**, 103801 (2020).
[20] G. D. Moore and D. Teaney, How much do heavy quarks thermalize in a heavy ion collision?, Phys. Rev. C **71**, 064904 (2005).
[21] H. van Hees, V. Greco, and R. Rapp, Heavy-quark probes of the quark-gluon plasma at RHIC, Phys. Rev. C **73**, 034913 (2006).
[22] S. Cao and S. A. Bass, Thermalization of charm quarks in infinite and finite QGP matter, Phys. Rev. C **84**, 064902 (2011).
[23] B. Svetitsky, Diffusion of charmed quarks in the quark-gluon plasma, Phys. Rev. D **37**, 2484 (1988).
[24] M. Golam Mustafa, D. Pal, and D. Kumar Srivastava, Propagation of charm quarks in equilibrating quark—gluon plasma, Phys. Rev. C **57**, 889 (1998); **57**, 3499(E) (1998).
[25] H. van Hees, M. Mannarelli, V. Greco, and R. Rapp, Nonperturbative heavy-quark diffusion in the quark-gluon plasma, Phys. Rev. Lett. **100**, 192301 (2008).
[26] S. Cao, G. Y. Qin, S. A. Bass, and B. Müller, Collisional vs. radiative energy loss of heavy quark in a hot and dense nuclear matter, Nucl. Phys. **A904–905**, 653c (2013).

[27] C. Young, B. Schenke, S. Jeon, and C. Gale, MARTINI event generator for heavy quarks: Initialization, parton evolution, and hadronization, Phys. Rev. C **86**, 034905 (2012).
[28] W. M. Alberico, A. Beraudo, A. De Pace, A. Molinari, M. Monteno, M. Nardi, and F. Prino, Heavy-flavour spectra in high energy nucleus-nucleus collisions, Eur. Phys. J. C **71**, 1666 (2011).
[29] Y. Akamatsu, T. Hatsuda, and T. Hirano, Heavy quark diffusion with relativistic Langevin dynamics in the quark-gluon fluid, Phys. Rev. C **79**, 054907 (2009).
[30] M. He, R. J. Fries, and R. Rapp, $\mathbf{D_s}$-meson as quantitative probe of diffusion and hadronization in nuclear collisions, Phys. Rev. Lett. **110**, 112301 (2013).
[31] A. Adare *et al.* (PHENIX Collaboration), Energy loss and flow of heavy quarks in $\mathrm{Au}+\mathrm{Au}$ collisions at $\sqrt{s}=200$ GeV, Phys. Rev. Lett. **98**, 172301 (2007).
[32] B. I. Abelev *et al.* (STAR Collaboration), Transverse momentum and centrality dependence of high-p_T non-photonic electron suppression in $\mathrm{Au}+\mathrm{Au}$ collisions at $\sqrt{s_{NN}}=200\,\mathrm{GeV}$, Phys. Rev. Lett. **98**, 192301 (2007); **106**, 159902(E) (2011).
[33] S. S. Adler *et al.* (PHENIX Collaboration), Nuclear modification of electron spectra and implications for heavy quark energy loss in $\mathrm{Au}+\mathrm{Au}$ collisions at $\sqrt{s_{NN}}=200$ GeV, Phys. Rev. Lett. **96**, 032301 (2006).
[34] B. Abelev *et al.* (ALICE Collaboration), Suppression of high transverse momentum D mesons in central Pb-Pb collisions at $\sqrt{s_{NN}}=2.76$ TeV, J. High Energy Phys. 09 (2012) 112.
[35] H. van Hees and R. Rapp, Thermalization of heavy quarks in the quark-gluon plasma, Phys. Rev. C **71**, 034907 (2005).
[36] V. Greco, C. M. Ko, and R. Rapp, Quark coalescence for charmed mesons in ultrarelativistic heavy ion collisions, Phys. Lett. B **595**, 202 (2004).
[37] V. Greco, C. M. Ko, and P. Levai, Parton coalescence and anti-proton / pion anomaly at RHIC, Phys. Rev. Lett. **90**, 202302 (2003).
[38] P. B. Gossiaux and J. Aichelin, Towards an understanding of the RHIC single electron data, Phys. Rev. C **78**, 014904 (2008).
[39] S. Plumari, W. M. Alberico, V. Greco, and C. Ratti, Recent thermodynamic results from lattice QCD analyzed within a quasi-particle model, Phys. Rev. D **84**, 094004 (2011).
[40] H. Berrehrah, P. B. Gossiaux, J. Aichelin, W. Cassing, and E. Bratkovskaya, Dynamical collisional energy loss and transport properties of on- and off-shell heavy quarks in vacuum and in the quark gluon plasma, Phys. Rev. C **90**, 064906 (2014).
[41] S. Cao, T. Luo, G. Y. Qin, and X. N. Wang, Linearized Boltzmann transport model for jet propagation in the quark-gluon plasma: Heavy quark evolution, Phys. Rev. C **94**, 014909 (2016).
[42] M. Djordjevic and M. Djordjevic, Generalization of radiative jet energy loss to non-zero magnetic mass, Phys. Lett. B **709**, 229 (2012).
[43] P. B. Gossiaux, J. Aichelin, T. Gousset, and V. Guiho, Competition of heavy quark radiative and collisional energy loss in deconfined matter, J. Phys. G **37**, 094019 (2010).
[44] S. K. Das, J. e. Alam, and P. Mohanty, Dragging heavy quarks in quark gluon plasma at the large hadron collider, Phys. Rev. C **82**, 014908 (2010).
[45] Y. L. Dokshitzer and D. E. Kharzeev, Heavy quark colorimetry of QCD matter, Phys. Lett. B **519**, 199 (2001).
[46] R. Abir, U. Jamil, M. G. Mustafa, and D. K. Srivastava, Heavy quark energy loss and D-mesons in RHIC and LHC energies, Phys. Lett. B **715**, 183 (2012).
[47] E. Braaten and M. H. Thoma, Energy loss of a heavy fermion in a hot plasma, Phys. Rev. D **44**, 1298 (1991).
[48] E. Braaten and M. H. Thoma, Energy loss of a heavy quark in the quark—gluon plasma, Phys. Rev. D **44**, R2625 (1991).
[49] M. G. Mustafa, D. Pal, D. K. Srivastava, and M. Thoma, Radiative energy loss of heavy quarks in a quark gluon plasma, Phys. Lett. B **428**, 234 (1998).
[50] M. G. Mustafa, Energy loss of charm quarks in the quark-gluon plasma: Collisional versus radiative, Phys. Rev. C **72**, 014905 (2005).
[51] G. Y. Qin, J. Ruppert, C. Gale, S. Jeon, G. D. Moore, and M. G. Mustafa, Radiative and collisional jet energy loss in the quark-gluon plasma at RHIC, Phys. Rev. Lett. **100**, 072301 (2008).
[52] R. Ghosh, M. Y. Jamal, and M. Kurian, Impact of the chiral asymmetry and a magnetic field on the passage of an energetic test parton in a QCD medium, Phys. Rev. D **108**, 054035 (2023).
[53] L. Thakur, N. Haque, and H. Mishra, Heavy quarkonium moving in hot and dense deconfined nuclear matter, Phys. Rev. D **95**, 036014 (2017).
[54] L. Thakur, N. Haque, and Y. Hirono, Heavy quarkonia in a bulk viscous medium, J. High Energy Phys. 06 (2020) 071.
[55] J. Sebastian, M. Y. Jamal, and N. Haque, Liénard-Wiechert potential of a heavy quarkonium moving in QGP medium, Phys. Rev. D **107**, 054040 (2023).
[56] L. Thakur and Y. Hirono, Spectral functions of heavy quarkonia in a bulk-viscous quark gluon plasma, J. High Energy Phys. 02 (2022) 207.
[57] S. K. Das, V. Chandra, and J. e. Alam, Heavy-quark transport coefficients in a hot viscous quark–gluon plasma medium, J. Phys. G **41**, 015102 (2013).
[58] J. Hong, Heavy quark diffusion and radiation at intermediate momentum, Phys. Rev. C **109**, 024913 (2024).
[59] A. Shaikh, M. Kurian, S. K. Das, V. Chandra, S. Dash, and B. K. Nandi, Heavy quark transport coefficients in a viscous QCD medium with collisional and radiative processes, Phys. Rev. D **104**, 034017 (2021).
[60] A. Shaikh, S. Dash, and B. K. Nandi, Viscous QCD medium effects on the bottom quark transport coefficients, Eur. Phys. J. C **83**, 959 (2023).
[61] B. Singh, A. Abhishek, S. K. Das, and H. Mishra, Heavy quark diffusion in a Polyakov loop plasma, Phys. Rev. D **100**, 114019 (2019).
[62] B. Singh and H. Mishra, Heavy quark transport in a viscous semi QGP, Phys. Rev. D **101**, 054027 (2020).
[63] M. Ruggieri, Pooja, J. Prakash, and S. K. Das, Memory effects on energy loss and diffusion of heavy quarks in the quark-gluon plasma, Phys. Rev. D **106**, 034032 (2022).
[64] P. Khowal, S. K. Das, L. Oliva, and M. Ruggieri, Heavy quarks in the early stage of high energy nuclear collisions

at RHIC and LHC: Brownian motion versus diffusion in the evolving glasma, Eur. Phys. J. Plus **137**, 307 (2022).
[65] V. N. Gribov, Quantization of non-Abelian gauge theories, Nucl. Phys. **B139**, 1 (1978).
[66] D. Zwanziger, Local and renormalizable action from the Gribov horizon, Nucl. Phys. **B323**, 513 (1989).
[67] Y. L. Dokshitzer and D. E. Kharzeev, The Gribov conception of quantum chromodynamics, Annu. Rev. Nucl. Part. Sci. **54**, 487 (2004).
[68] N. Vandersickel and D. Zwanziger, The Gribov problem and QCD dynamics, Phys. Rep. **520**, 175 (2012).
[69] D. Dudal, J. A. Gracey, S. P. Sorella, N. Vandersickel, and H. Verschelde, A refinement of the Gribov-Zwanziger approach in the Landau gauge: Infrared propagators in harmony with the lattice results, Phys. Rev. D **78**, 065047 (2008).
[70] M. A. L. Capri, M. S. Guimaraes, I. F. Justo, L. F. Palhares, and S. P. Sorella, Properties of the Faddeev-Popov operator in the Landau gauge, matter confinement and soft BRST breaking, Phys. Rev. D **90**, 085010 (2014).
[71] M. A. L. Capri, D. Dudal, D. Fiorentini, M. S. Guimaraes, I. F. Justo, A. D. Pereira, B. W. Mintz, L. F. Palhares, R. F. Sobreiro, and S. P. Sorella, Exact nilpotent nonperturbative BRST symmetry for the Gribov-Zwanziger action in the linear covariant gauge, Phys. Rev. D **92**, 045039 (2015).
[72] M. A. L. Capri, D. Fiorentini, M. S. Guimaraes, B. W. Mintz, L. F. Palhares, S. P. Sorella, D. Dudal, I. F. Justo, A. D. Pereira, and R. F. Sobreiro, More on the nonperturbative Gribov-Zwanziger quantization of linear covariant gauges, Phys. Rev. D **93**, 065019 (2016).
[73] M. A. L. Capri, D. Dudal, D. Fiorentini, M. S. Guimaraes, I. F. Justo, A. D. Pereira, B. W. Mintz, L. F. Palhares, R. F. Sobreiro, and S. P. Sorella, Local and BRST-invariant Yang-Mills theory within the Gribov horizon, Phys. Rev. D **94**, 025035 (2016).
[74] D. Dudal, C. P. Felix, L. F. Palhares, F. Rondeau, and D. Vercauteren, The BRST-invariant vacuum state of the Gribov–Zwanziger theory, Eur. Phys. J. C **79**, 731 (2019).
[75] D. Dudal, C. P. Felix, M. S. Guimaraes, and S. P. Sorella, Accessing the topological susceptibility via the Gribov horizon, Phys. Rev. D **96**, 074036 (2017).
[76] E. Gotsman and E. Levin, Gribov-Zwanziger confinement, high energy evolution, and large impact parameter behavior of the scattering amplitude, Phys. Rev. D **103**, 014020 (2021).
[77] E. Gotsman, Y. Ivanov, and E. Levin, High energy evolution for Gribov-Zwanziger confinement: Solution to the equation, Phys. Rev. D **103**, 096017 (2021).
[78] I. F. Justo, A. D. Pereira, and R. F. Sobreiro, Toward background field independence within the Gribov horizon, Phys. Rev. D **106**, 025015 (2022).
[79] J. A. Gracey, Alternative refined Gribov-Zwanziger Lagrangian, Phys. Rev. D **82**, 085032 (2010).
[80] M. Tissier and N. Wschebor, Infrared propagators of Yang-Mills theory from perturbation theory, Phys. Rev. D **82**, 101701 (2010).
[81] B. W. Mintz, L. F. Palhares, G. Peruzzo, and S. P. Sorella, Infrared massive gluon propagator from a BRST-invariant Gribov horizon in a family of covariant gauges, Phys. Rev. D **99**, 034002 (2019).
[82] M. Peláez, U. Reinosa, J. Serreau, M. Tissier, and N. Wschebor, A window on infrared QCD with small expansion parameters, Rep. Prog. Phys. **84**, 124202 (2021).
[83] K. Fukushima and N. Su, Stabilizing perturbative Yang-Mills thermodynamics with Gribov quantization, Phys. Rev. D **88**, 076008 (2013).
[84] N. Su and K. Tywoniuk, Massless mode and positivity violation in hot QCD, Phys. Rev. Lett. **114**, 161601 (2015).
[85] D. E. Kharzeev and E. M. Levin, Color confinement and screening in the θ vacuum of QCD, Phys. Rev. Lett. **114**, 242001 (2015).
[86] W. Florkowski, R. Ryblewski, N. Su, and K. Tywoniuk, Transport coefficients of the Gribov-Zwanziger plasma, Phys. Rev. C **94**, 044904 (2016).
[87] W. Florkowski, R. Ryblewski, N. Su, and K. Tywoniuk, Bulk viscosity in a plasma of Gribov-Zwanziger gluons, Acta Phys. Pol. B **47**, 1833 (2016).
[88] A. Jaiswal and N. Haque, Covariant kinetic theory and transport coefficients for Gribov plasma, Phys. Lett. B **811**, 135936 (2020).
[89] A. Bandyopadhyay, N. Haque, M. G. Mustafa, and M. Strickland, Dilepton rate and quark number susceptibility with the Gribov action, Phys. Rev. D **93**, 065004 (2016).
[90] Sumit, N. Haque, and B. K. Patra, QCD mesonic screening masses using Gribov quantization, Phys. Lett. B **845**, 138143 (2023).
[91] A. Bandyopadhyay, Electromagnetic Debye mass within Gribov-Zwanziger action, arXiv:2307.09656.
[92] W. Wu, G. Huang, J. Zhao, and P. Zhuang, Heavy-quark potential in the Gribov-Zwanziger approach around the deconfinement phase transition, Phys. Rev. D **107**, 114033 (2023).
[93] M. Debnath, R. Ghosh, and N. Haque, The complex heavy quarkonium potential with the Gribov–Zwanziger action, Eur. Phys. J. C **84**, 313 (2024).
[94] M. Debnath, R. Ghosh, M. Y. Jamal, M. Kurian, and J. Prakash, Energy loss of a fast moving parton in Gribov-Zwanziger plasma, Phys. Rev. D **109**, L011503 (2024).
[95] S. Madni, A. Mukherjee, A. Bandyopadhyay, and N. Haque, Estimation of the diffusion coefficient of heavy quarks in light of Gribov-Zwanziger action, Phys. Lett. B **838**, 137714 (2023).
[96] S. Mazumder, T. Bhattacharyya, J. e. Alam, and S. K. Das, Momentum dependence of drag coefficients and heavy flavour suppression in quark gluon plasma, Phys. Rev. C **84**, 044901 (2011).
[97] S. Mazumder, T. Bhattacharyya, and J.-e. Alam, Gluon bremsstrahlung by heavy quarks—its effects on transport coefficients and equilibrium distribution, Phys. Rev. D **89**, 014002 (2014).
[98] A. Kumar, M. Kurian, S. K. Das, and V. Chandra, Drag of heavy quarks in an anisotropic QCD medium beyond the static limit, Phys. Rev. C **105**, 054903 (2022).
[99] T. Matsui, B. Svetitsky, and L. D. McLerran, Strangeness production in ultrarelativistic heavy ion collisions. 1. Chemical kinetics in the quark—gluon plasma, Phys. Rev. D **34**, 783 (1986).
[100] X. N. Wang, M. Gyulassy, and M. Plumer, The LPM effect in QCD and radiative energy loss in a quark gluon plasma, Phys. Rev. D **51**, 3436 (1995).

[101] M. Gyulassy and X. n. Wang, Multiple collisions and induced gluon bremsstrahlung in QCD, Nucl. Phys. **B420**, 583 (1994).
[102] S. Klein, Suppression of bremsstrahlung and pair production due to environmental factors, Rev. Mod. Phys. **71**, 1501 (1999).
[103] R. Abir, C. Greiner, M. Martinez, M. G. Mustafa, and J. Uphoff, Soft gluon emission off a heavy quark revisited, Phys. Rev. D **85**, 054012 (2012).
[104] N. Haque, A. Bandyopadhyay, J. O. Andersen, M. G. Mustafa, M. Strickland, and N. Su, Three-loop HTLpt thermodynamics at finite temperature and chemical potential, J. High Energy Phys. 05 (2014) 027.
[105] S. Borsanyi, G. Endrodi, Z. Fodor, S. D. Katz, and K. K. Szabo, Precision SU(3) lattice thermodynamics for a large temperature range, J. High Energy Phys. 07 (2012) 056.
[106] B. Müller, $\eta/s - \hat{q}/T^3$ relation at next-to-leading order in QCD, Phys. Rev. D **104**, L071501 (2021).
[107] P. Kovtun, D. T. Son, and A. O. Starinets, Viscosity in strongly interacting quantum field theories from black hole physics, Phys. Rev. Lett. **94**, 111601 (2005).
[108] S. Madni, A. Mukherjee, A. Jaiswal, and N. Haque, Shear and bulk viscosity of quark-gluon plasma with Gribov gluons and quasiparticle quarks, arXiv:2401.08384.
[109] S. Madni, L. Thakur, and N. Haque, Electrical conductivity of QGP with quasiparticle quarks and Gribov gluon, arXiv:2404.09767.
[110] J. Prakash, M. Kurian, S. K. Das, and V. Chandra, Heavy quark transport in an anisotropic hot QCD medium: Collisional and radiative processes, Phys. Rev. D **103**, 094009 (2021).
[111] P. K. Srivastava and B. K. Patra, Drag and diffusion of heavy quarks in a hot and anisotropic QCD medium, Eur. Phys. J. A **53**, 116 (2017).
[112] J. Prakash, V. Chandra, and S. K. Das, Heavy quark radiation in an anisotropic hot QCD medium, Phys. Rev. D **108**, 096016 (2023).
[113] M. Singh, M. Kurian, S. Jeon, and C. Gale, Open charm phenomenology with a multistage approach to relativistic heavy-ion collisions, Phys. Rev. C **108**, 054901 (2023).
[114] K. Fukushima, K. Hattori, H. U. Yee, and Y. Yin, Heavy quark diffusion in strong magnetic fields at weak coupling and implications for elliptic flow, Phys. Rev. D **93**, 074028 (2016).
[115] A. Bandyopadhyay, J. Liao, and H. Xing, Heavy quark dynamics in a strongly magnetized quark-gluon plasma, Phys. Rev. D **105**, 114049 (2022).
[116] A. Bandyopadhyay, Heavy quark diffusion coefficients in magnetized quark-gluon plasma, Phys. Rev. D **109**, 034013 (2024).